

Antihydrogen from merged plasmas - cold enough to trap?

Niels Madsen¹

Department of Physics, University of Wales Swansea, Swansea SA2 8PP, United Kingdom

Abstract. The merging of antiprotons with a positron plasma is the predominant and highest efficient method for cold antihydrogen formation used to date [1, 2, 3]. We present experimental evidence that this method has serious disadvantages for producing antihydrogen cold enough to be trapped [4, 5]. Antihydrogen is neutral but may be trapped in a magnetic field minimum. However, the depth of such traps are of order 1 K, shallow compared to the kinetic energies in current antihydrogen experiments. Studying the spatial distribution of the antihydrogen emerging from the ATHENA positron plasma we have, by comparison with a simple model, extracted information about the temperature of the antihydrogen formed. We find that antihydrogen is formed before thermal equilibrium is attained between the antiprotons and the positrons, and thus that further positron cooling may not be sufficient for producing antihydrogen cold enough to be trapped [5]. We discuss the implications for trapping of antihydrogen in a magnetic trap, important for ongoing work by the ALPHA collaboration [6].

Keywords: Antihydrogen, Non-neutral Plasma, Cold Plasma, Magnetic Trap

PACS: 36.10.-k, 34.80.Lx, 52.20.Hv

INTRODUCTION

Cold Antihydrogen was first produced by the ATHENA and ATRAP collaborations, both at CERN, in 2002 [1, 2]. This milestone is important for the long-term goal of making precision comparisons of hydrogen and antihydrogen in order to test fundamental symmetries. However, with production rates averaging ~ 10 Hz at best [3], it seems to be a precondition for success that antihydrogen be trapped so as to increase interaction times as well as numbers. It is therefore the immediate goal of both the newly formed ALPHA collaboration (an offspring of the former ATHENA collaboration) [6] and the ATRAP collaboration to trap antihydrogen. Using current technology this can only be done in a magnetic minimum trap, trapping the antiatoms on their magnetic dipole moment. Such traps are intrinsically shallow, in the sense that their depth is about 0.7 K/Tesla.

One particular goal that both the ALPHA and ATRAP collaborations have in mind is the precision comparison of the 1s-2s two-photon transition in hydrogen and antihydrogen. This comparison may benefit from the impressive precision achieved in measuring this transition in hydrogen [7]. To achieve this the main intermediate goal is to create large amounts of trapped, cold antihydrogen in its positronic ground state.

To date most of the antihydrogen, and in particular that produced with the rate indicated above, has been synthesized using the so-called nested-trap scheme. This is a

¹ On behalf of the ALPHA and ATHENA collaborations. Contact : N.Madsen@swansea.ac.uk

variation of the traditional Penning-Malmberg trap that allows for the simultaneous confinement of both positrons and antiprotons in the same spatial region [8]. We have found that antihydrogen is formed before the antiprotons, that are cooled by the positrons, have reached thermal equilibrium with the positrons [5]. This results in antihydrogen that is far warmer than initially expected, and means that simply cooling down the positrons further will not result in a huge increase in antihydrogen cold enough to be trapped. In this paper we discuss the reasons for this, and alternative schemes of formation that may resolve the issue.

FORMATION OF ANTIHYDROGEN IN ATHENA

Antiprotons for antihydrogen production were supplied by the CERN AD in spills of $2\text{-}3 \times 10^7$ antiprotons every ~ 100 s. Those were degraded in a foil, and antiprotons with energy less than 5 keV were dynamically trapped in a Penning-Malmberg trap, where their radial motion was confined by a 3 T superconducting solenoid magnetic field. The antiprotons were then cooled by collisions with a batch of pre-loaded electrons. The electrons cooled by emission of synchrotron radiation to near the ambient temperature of the trap of 15 K. A number of AD spills could be accumulated, and it was usual to accumulate 2-3 spills which resulted in $1\text{-}2 \times 10^4$ cold and trapped antiprotons for antihydrogen formation.

Positrons were obtained from a 40 mCi ^{22}Na source and immediately moderated by a frozen neon film. Trapping, cooling and accumulation was achieved using a nitrogen buffer gas, which provided the dissipative process for trapping the continuous flow of positrons. The method was pioneered by Surko and co-workers [9]. Around 150 million positrons were accumulated in a 0.14 T field every 5 min. after which they were transferred to the 3 T field with about 45% transfer efficiency. The transfer could be repeated and the positrons accumulated in the high field, in this way a record number of positrons of $> 1.2 \times 10^9$ was accumulated. In the high B-field Penning trap a rotating electric field (so-called rotating wall) could also be applied which would compress the positron plasma [10]. A record density of $2.6 \times 10^{10} \text{ cm}^{-3}$ was achieved in this way [11].

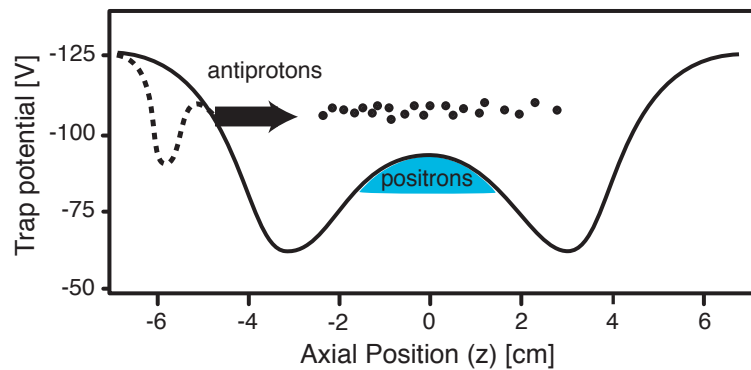


FIGURE 1. Nested trap configuration of the mixing trap for mixing positrons and antiprotons for antihydrogen formation. The potential on axis is given. The dashed curve indicates the potential before injection of the antiprotons.

Antihydrogen formation took place in the so-called mixing trap, which was a double trap, where the positrons were housed in an inverted well at the center of the antiproton trap (Figure 1). This configuration is referred to as a nested trap [8]. Antihydrogen production was carried out by first loading the mixing trap with $\sim 7 \times 10^7$ positrons, which cooled to the ambient temperature by the emission of synchrotron radiation, and then injecting about 10^4 antiprotons into the nested region where they interacted through the Coulomb interaction with the positron plasma. The antiprotons were thus cooled by the positron plasma, and eventually, when the relative velocities were sufficiently low they could combine and form antihydrogen. This cooling process was first demonstrated by Gabrielse et al. [12], but with only 1/4 million positrons. Figure 2 shows how the antiprotons lose energy when cooled by 70 million positrons [4]. When antiprotons are mixed with ambient temperature positrons it is referred to as "cold" mixing. Alternatively the positron plasma could be heated by RF excitation to suppress antihydrogen formation [13]. Mixing with plasmas where the temperature has been increased by ~ 3500 K is termed "hot" mixing.

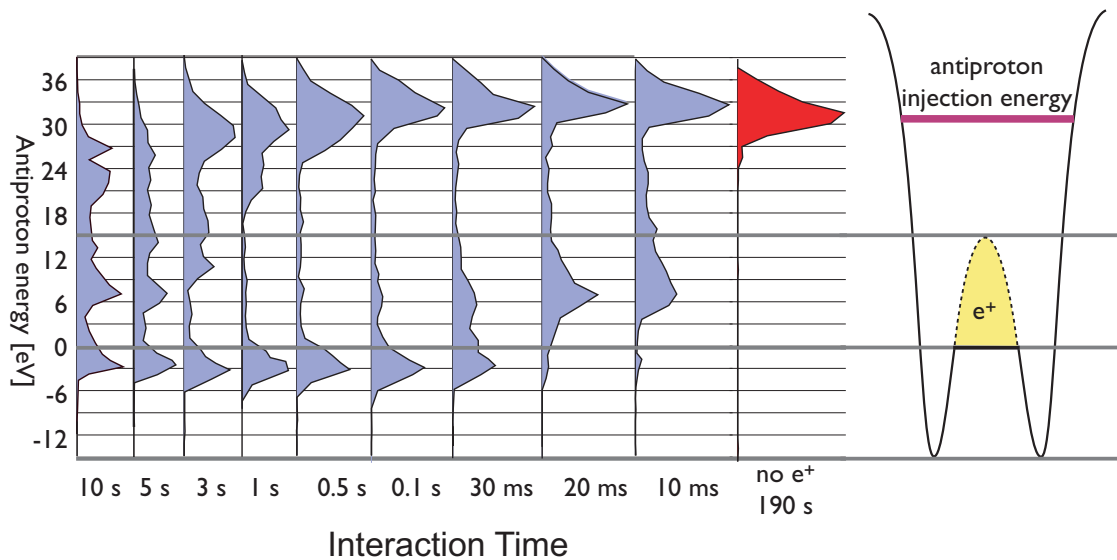


FIGURE 2. Antiproton energy distribution as a function of mixing time with positrons in a nested trap. The energy distributions were measured by lowering the left trap wall and monitoring the number of antiprotons escaping as a function of the trap voltage by letting them annihilate on the degrader. Note that when no positrons are present, the antiprotons remain at their initial injection energy, about 15 eV above the level of the positrons. With positrons we observe how the antiprotons are cooled, and how some of them manage to end up with too little energy to be able to enter the positron plasma (they become trapped in the side wells) [17].

In a typical measurement the antiprotons interacted with the positron plasma for about 180 s. before both species were ejected and the cycle restarted. The neutral antihydrogen atoms drifted away from the formation region until they annihilated on the electrodes of the mixing trap. The antihydrogen detector could observe charged particle tracks using two layers of double-sided silicon microstrip detectors, and from these the vertices of antiproton annihilations could be reconstructed with a precision of ~ 4 mm (1σ). The detector also observed the back-to-back 511 keV photons from the annihilation of positrons by highly segmented pure CsI crystals read out by avalanche photodiodes [14].

IMAGING ANTIHYDROGEN ANNIHILATIONS

In the first demonstration of antihydrogen formation, spatial and temporal coincidence between the antiproton and the positron annihilations was used to demonstrate the formation of antihydrogen. However, the photon detection efficiency was quite low, and it was soon shown that the initially detected 131 ± 22 antihydrogen atoms (with full reconstruction of the event) corresponded to about 1/4 million antihydrogen atoms formed [3].

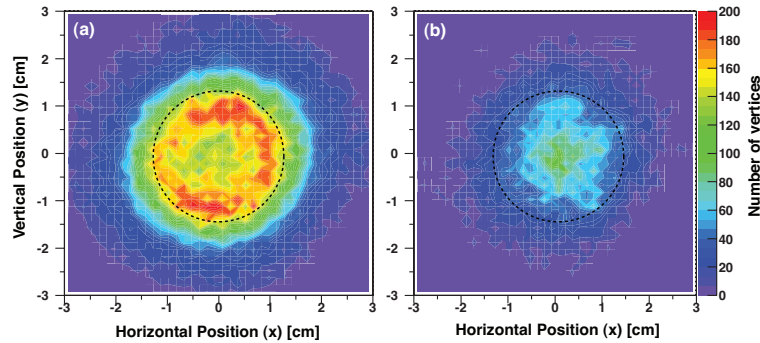


FIGURE 3. Cross sectional distribution (xy) of all antiproton annihilation vertices registered during cold (a) and hot (b) mixing. The black dashed circles mark the position of the trap walls. The cylindrical traps have a diameter of 25 mm.

Figure 3 shows the cross-sectional (xy) distribution of all antiproton annihilations (no cuts applied) registered during cold and hot mixing respectively. The distinct difference between Figure 3.a and Figure 3.b is the enhancement of annihilations at the trap wall during cold mixing. Using the hot mixing as a background with no antihydrogen assumed it was found that the efficiency for antihydrogen formation was about 15% of the mixed antiprotons. A few percent of the antiprotons annihilated on rest gas or positive ions trapped by the positron plasma, whereas the bulk of the antiprotons remained in the trap but in regions decoupled either axially (in the side wells of the nested-trap) or radially from the positron plasma as evidenced in the measurements in Figure 2 [4].

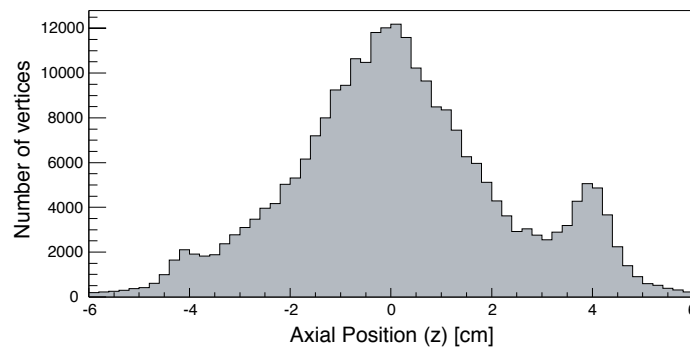


FIGURE 4. Axial distribution of antiproton annihilation vertices during cold mixing.

A powerful way to distinguish antihydrogen annihilations on the wall from antiproton-only annihilations arose from the observation that antiprotons annihilating on the walls

annihilate in an azimuthally asymmetric way. Particles trapped in a Penning trap are, if nothing is done to actively prevent it, radially transported towards the walls of the trap where they will be lost. The rate of transport depends on a range of parameters of the system. However, it was observed using the antihydrogen detector that the losses are always localized, both axially and azimuthally [15]. Figure 4 shows a typical axial annihilation distribution from cold mixing. The left and the right peaks can be associated with antiproton-only losses as they are azimuthally localized as shown in Figure 5. The central structure is composed of about 65% antihydrogen and 35% antiproton annihilations on rest gas or ions and is azimuthally symmetric.

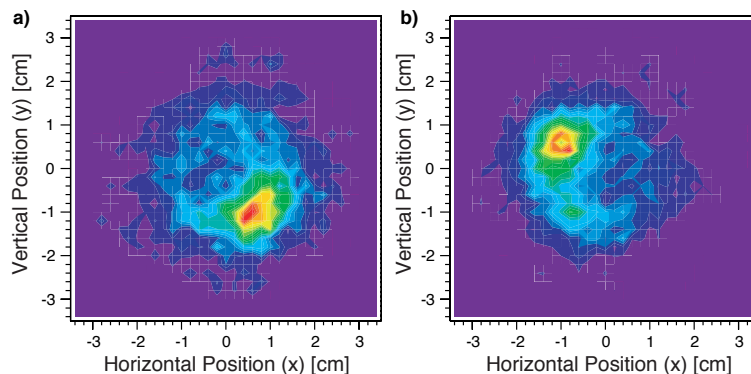


FIGURE 5. Cross sectional distributions of vertices from the two size peaks in Figure 4. (a) Left peak $-4.5 < z < -3.5$. (b) Right peak $3.5 < z < 4.5$.

ANTIHYDROGEN TEMPERATURE

Antihydrogen is formed when a positron is bound to an antiproton. The neutral antihydrogen, once formed, was not confined by the ATHENA trap and drifted unhindered until it annihilated, typically on the trap electrodes. The distribution of antihydrogen annihilations on the trap wall was used to extract information about the temperature of the antihydrogen [5].

The cross-section signature of antihydrogen is an isotropic distribution of events on the electrodes. The axial distribution however will depend on the velocities, that is the temperature, of the antiatoms formed. Figure 6 shows the axial distribution of antihydrogen annihilations on the wall for three different temperatures of the positron plasma. No dependence on the temperature can be seen. In the figure the distributions are compared to a simple isotropic emission distribution where it is assumed that antihydrogen is from all positions within the positron plasma. There is poor agreement between the measurements and this naive picture.

To understand the spatial distribution, and to try to extract temperature information from it we developed a simple model for how the annihilation distribution is formed [5]. At thermal equilibrium the positron plasma $\mathbf{E} \times \mathbf{B}$ rotates with a frequency that for typical ATHENA parameters was about 80 kHz, corresponding to a surface velocity of $1.3 \times 10^3 \text{ m s}^{-1}$. An antiproton in the radial field of the positrons at the surface of the plasma will $\mathbf{E} \times \mathbf{B}$ drift with the same velocity. The thermal velocity of 15 K antiprotons

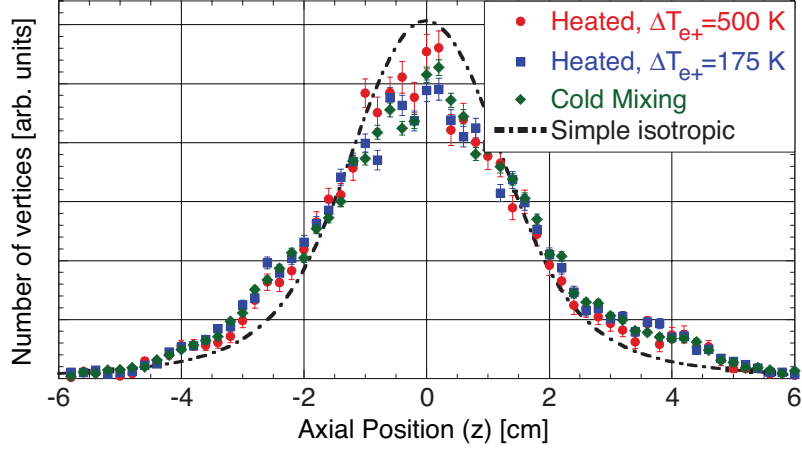


FIGURE 6. Axial antihydrogen distributions for cold mixing and mixing with positrons heated by two different amounts (hot mixing subtracted, hot spots removed). The dot-dashed line is a simple calculation of isotropic emission from the positron plasma volume. The distributions have been normalized to the same area.

is $\sim 350 \text{ m s}^{-1}$. The drift contribution to the antiproton, and therefore the antihydrogen, velocity can therefore be significant.

We modeled the axial distribution by randomly distributing antihydrogen in a selected formation volume and assigning to each antihydrogen a velocity from a three dimensional Gaussian velocity distribution characterized by transverse ($T_{\bar{p}}^{\perp}$) and axial ($T_{\bar{p}}^{\parallel}$) temperatures and adding an azimuthal velocity given by the radial position of the antiatom. We used two different temperatures to be able to describe non-equilibrium conditions. The intersection of the antihydrogen's undisturbed path with the cylindrical electrodes was then calculated. Then the vertex reconstruction resolution of the detector ($\sigma = 4 \text{ mm}$), and the response function were folded onto the result. The antiprotons will, due to their mass, dominate the momentum of the antihydrogen atoms and we therefore neglected the positron temperature in this model. We assumed that antihydrogen was formed homogeneously throughout the rotating ellipsoidal positron plasma.

Figure 7 shows a number of calculated distributions using the model described above. Also shown is the measured cold mixing distribution. If we assume thermal equilibrium between the positrons and the antiprotons we have a huge disagreement between the model and the observations (dotted curve). However, if we assume $T_{\bar{p}}^{\perp} = 15 \text{ K}$, the model matches the observed cold mixing distribution with $T_{\bar{p}}^{\parallel} = (10 \pm 2) \times T_{\bar{p}}^{\perp}$ (solid curve in Figure 7). This gives a lower limit of $T_{\bar{p}}^{\parallel} = 150 \text{ K}$. The antiprotons which form antihydrogen are therefore not in thermal equilibrium with the positrons. We cannot determine the temperature ($T_{\bar{p}}$) of the antiprotons that form antihydrogen from these measurements. However, as we increase $T_{\bar{p}}^{\perp}$ the necessary difference between the $T_{\bar{p}}^{\parallel}$ and $T_{\bar{p}}^{\perp}$ to model the observations decreases asymptotically to a factor 2.3 ± 0.6 (shown in Figure 7). This is because the influence of $\mathbf{E} \times \mathbf{B}$ rotation on the distribution decreases with increasing temperature. Thus, even with no influence from $\mathbf{E} \times \mathbf{B}$ rotation we

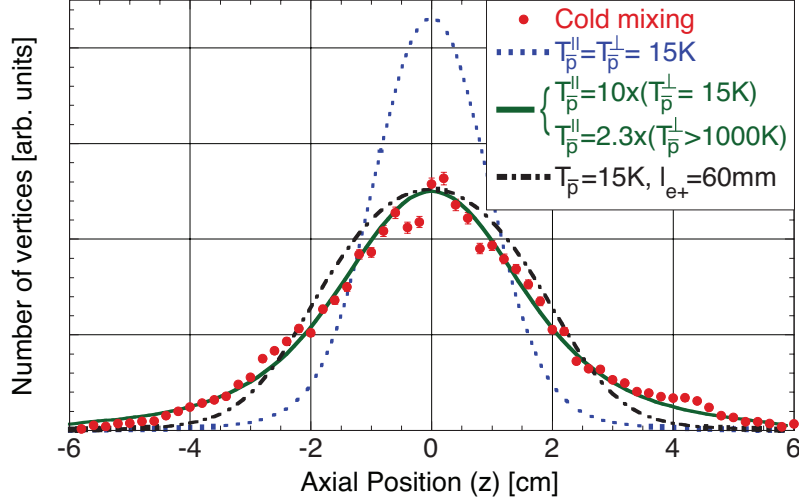


FIGURE 7. Comparison of the axial distribution from cold mixing with a number of calculated distributions (see text for details). Standard positron plasma parameters and $\mathbf{E} \times \mathbf{B}$ rotation were used except for the dot-dashed curve where the positron plasma length was set to an unrealistic 60 mm (longer than the actual trap). Homogeneous formation in the plasma was assumed.

cannot find consistency with thermal equilibrium, i.e. our conclusion is independent of the absolute positron temperature. Comparing the model distributions we find that for $T_{\bar{p}} > 10^3$ K the influence of the $\mathbf{E} \times \mathbf{B}$ rotation is negligible. If the positron temperature $T_{e^+} < 10^3$ K, and the antiprotons are in thermal equilibrium with the positrons, the antihydrogen distribution should thus change when the positrons are heated. We observe no change (Figure 6) also indicating that the antiprotons forming antihydrogen are not in thermal equilibrium with the positrons. This behavior also excludes the interesting idea that polarized antihydrogen may, under special circumstances, be trapped by the radial electric field of the positron plasma [16].

That antihydrogen is formed before thermal equilibrium between antiprotons and positrons is achieved indicates that the formation rate is high compared to the antiproton cooling rate. The formation rate is expected to scale inversely with some power of the relative velocity [17]. In the literature this rate is often given as a function of the temperature, as thermal equilibrium between the particle species, is assumed. Due to the much larger mass of the antiproton the relative velocity is however dominated by the positron velocity as long as $T_{\bar{p}} < 2000 \times T_{e^+}$. For $T_{e^+} = 15$ K this is equivalent to $T_{\bar{p}} = 30000$ K or an antiproton kinetic energy of 2.6 eV. The antiproton injection energy was ~ 15 eV. For comparison, an estimate of the 3-body formation rate using Ref. [18], using 10^4 antiprotons and ATHENA positron plasma parameters gives a rate of ~ 8 kHz at a temperature of 30 K, roughly equivalent to the relative velocities of 30000 K antiprotons interacting with 15 K positrons. This rate is very high compared to the cooling rate and allows many antiprotons to form antihydrogen at high temperature. Recent simulations by Robicheaux also indicate that antihydrogen is formed with high axial momentum (i.e. high $T_{\bar{p}}^{\parallel}$) [19]. The observed temperatures are incompatible with trapping in a magnetic minimum trap.

ANTIHYDROGEN STATE

The positronic state of the antihydrogen is important for the trapping of the antihydrogen, as the well depth of the magnetic trap depends on the magnetic moment. Furthermore it is important to have antihydrogen in its ground state as a basis for spectroscopy. The state of the formed antihydrogen depends on the formation mechanism. It is therefore important to identify and possibly control the mechanism through which antihydrogen is formed. This section describes experiments performed by ATHENA to identify and control the state of the bulk of the antihydrogen formed.

By applying a resonant RF field to excite the dipole mode of the positron plasma it can be heated [13]. Using this feature ATHENA studied the temperature dependence of the formation of antihydrogen [17]. Figure 8 shows the dependence of the peak trigger rate and the total number of triggers (backgrounds subtracted) as a function of the positron plasma temperature. These numbers have been shown to be good proxies for antihydrogen formation [3].

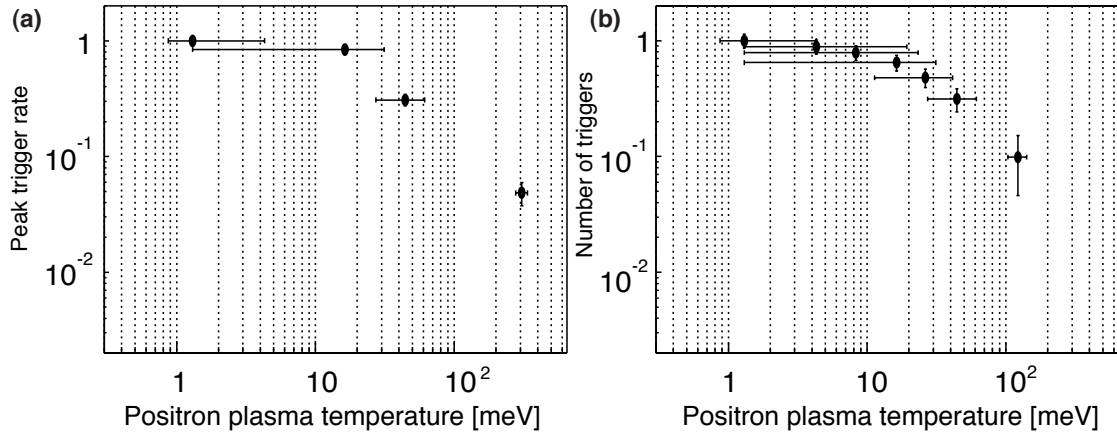


FIGURE 8. Formation dependence on positron temperature. (a) The peak detector trigger rate dependence. (b) The dependence of the total number of triggers in a mixing cycle.

One expects two processes to be the main contributors to the formation in the present experimental conditions [20]. They are radiative formation, where a photon carries away the excess energy and momentum and 3-body formation where an additional positron carries it away [21, 22, 23]. The radiative process is expected to scale as $T_{e^+}^{-0.63}$ in zero magnetic field [23] and the 3-body process as $T_{e^+}^{-9/2}$ [18]. These calculations assume thermal equilibrium between the positrons and the antiprotons, which means that the antiproton temperature can be ignored as antiprotons are much heavier than positrons.

The measurements in Figure 8 show that the formation changes slowly with temperature for low temperatures and at around room temperature (~ 26 meV) the formation decreases as $\sim T_{e^+}^{-0.7}$. The expected strong rise in the formation at low temperatures where the 3-body process should dominate is thus absent. The persistence of formation at high temperature could indicate some radiative contribution. However, the total measured rates are about a factor of 10 higher than a naive radiative calculation, neglecting the magnetic field, would suggest. Furthermore, our direct comparisons with the equilibrium rates is somewhat naive, as what was measured was not a pure measurement of

the temperature dependence of the formation. Antihydrogen may be field-ionized before reaching the wall if it has been formed in a sufficiently weakly bound state. Including the space charge field of the positrons the minimum field that an antihydrogen had to survive to escape to annihilate on the trap walls was about 35 V cm^{-1} . This would be enough to field-ionize all atoms bound weaker than about 4.5 meV. As the distribution of final states depend on temperature, the amount of "screening" performed by the electric fields will depend on the positron temperature. Recent work by Robicheaux has addressed some of these issues through simulations [19, 24]. With these effects in mind, it is clear that the direct comparison with equilibrium rates is relatively naive. However, the observation that the rates are much higher than radiative formation rates strongly suggests that antihydrogen formation is predominantly happening through the three-body process. This agrees with the previous evidence that antihydrogen is not formed at thermal equilibrium.

As a starting point for spectroscopy the antihydrogen will have to be in its ground state. We therefore attempted to laser-stimulate the radiative formation of antihydrogen using a 50 W $^{13}\text{C}^{18}\text{O}_2$ laser which should couple the continuum and the $n = 11$ state in antihydrogen, where n is the principal quantum number. We expected rapid decay from this state, should it be reached, to the ground state. The experiment was inspired by Ref. [25]. The result of the experiment was essentially null, i.e. we saw no influence of the laser on the formation, neither negative nor positive. Barring the unlikely case of experimental error, this result supports the hypothesis that we are dominated by three-body recombination in a situation without thermal equilibrium between antiprotons and positrons [26].

ALTERNATIVE FORMATION SCHEMES

In the preceding sections we have seen that the standard nested-trap based scheme for producing antihydrogen tends to produce antihydrogen that is significantly warmer than the ambient temperature. The main cause seems to be that the formation mechanism is much faster than the cooling, which results in positrons recombining with antiprotons before they have cooled the antiprotons to the ambient temperature. As the antiprotons contribute most of the momentum to the antihydrogen, it is crucial for making cold antihydrogen that antiprotons are cold when they recombine. Figure 9 shows ideas for variations of the nested-trap scheme for creating cold, trapable antihydrogen and which will be attempted by the ALPHA experiment [6].

We have seen that under the conditions used by ATHENA the antiprotons tended to accumulate in the side-wells without further possibility to combine with positrons (Figure 2). As no dissipative mechanism seems to be responsible, this separation is likely to be caused by field-ionization of weakly bound antihydrogen. As the field is the strongest at the trap sides, the antiprotons are trapped with a large energy in the side-wells, and they are therefore very close to the positron level (probably some are even naturally recycled this way). Thus, by lowering the positron energy relative to the side wells or pushing the antiprotons slowly into the positron plasma from the side wells we can obtain antihydrogen from antiprotons with a low kinetic energy (Figure 9.a). A variation of this is to initially inject the antiprotons at low relative energy to the

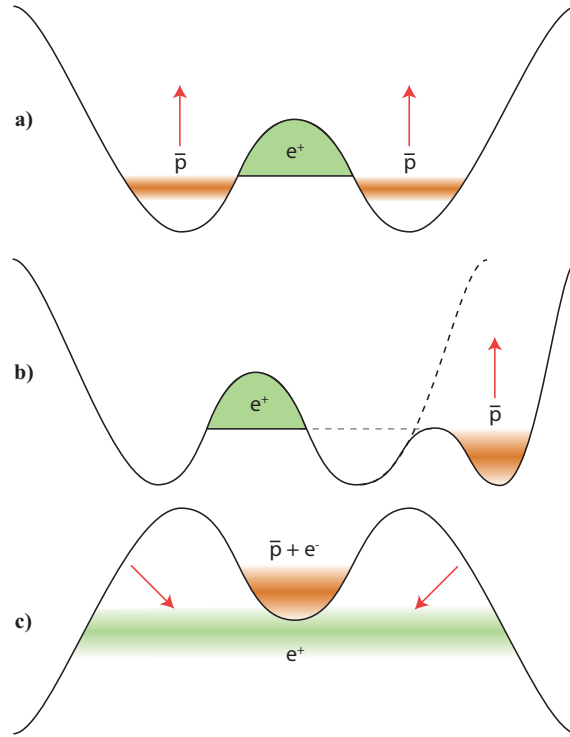


FIGURE 9. Examples of suggested mixing schemes for creating antihydrogen cold enough to trap. a) The antiprotons that accumulate in the sidewells may be slowly reinjected to interact with the positrons at low relative energies. b) The initial injection of antiprotons may be attempted at low relative energy, possibly directly from the sidewell with electrons to keep the antiprotons cold. c) The antiprotons are kept cold while the positrons are injected.

positrons, and not at 15 eV as was typically used in ATHENA (Figure 9.b). However, the antiprotons are initially mixed with electrons to cool them to the ambient temperature, and ejecting the electrons inevitably heats the antiprotons. One suggestion is therefore to keep enough electrons with the antiprotons that they stay cold, and then let the electron-antiproton mixture into the positron plasma, where the electrons may cause positronium to be formed, which could possibly be an advantage for the formation of antihydrogen. A different approach is to invert the nested scheme and keep the antiprotons cold with electrons in the center and inject the positrons. However, the positrons will cool into the side wells and will have to be re-injected repeatedly (Figure 9.c).

An alternative route to cold antihydrogen is to go via positronium as first suggested by Humberston *et al.* [27]. An indirect scheme using positronium was recently demonstrated by Storry *et al.* [28], but the formation rates were very low compared to the nested scheme .

Finally, it should be pointed out that the space-charge induced $\mathbf{E} \times \mathbf{B}$ rotation of the antiprotons, by either a positron or an electron plasma, puts an upper limit on the densities that can be used to make trappable antihydrogen. In a simple calculation we find that if antihydrogen is formed at 4K in a 1 T axial field and the magnetic trap depth is 0.5 K, the trappable fraction is only 5×10^{-4} with a typical ATHENA positron plasma

with a density of $1.7 \times 10^8 \text{ cm}^{-3}$. This issue could possibly be resolved if the antiprotons can be maintained very near the axis, where the rotation is minimal. This can perhaps be done by using the aforementioned rotating-wall technique, or alternatively by applying so-called side-band cooling as developed by ATHENA [29].

SUMMARY

We have presented experimental evidence from the ATHENA experiment that shows that antihydrogen formed using the standard nested-trap scheme for mixing antiprotons and positrons is predominantly formed through the three-body mechanism and is too warm to be trapped in state-of-the-art magnetic traps. The main reason for this is that the formation rate is dominated by the relative velocity, which, as the positrons are quite light compared to the antiprotons, is dominated by the positron temperature. However, the antihydrogen temperature is essentially given by the temperature of the antiproton at the time of formation. As the antiprotons are cooled by the positrons, and this process is relatively slow, they have plenty of opportunity to form antihydrogen before they have reached thermal equilibrium, and this is essentially what happens.

ALPHA is a new experiment that aims to trap antihydrogen in a superconducting magnetic trap. These results are therefore of crucial importance, and we discussed some of the approaches planned by ALPHA in order to form antihydrogen cold enough to be trapped. The central common feature of the various ALPHA ideas is that the antiprotons must be cold when they combine with the positrons.

ACKNOWLEDGMENTS

The author wishes to acknowledge the support of the Danish National Research Foundation and the EPSRC, UK. Furthermore the ATHENA and ALPHA collaborations are or have been supported by FAPERJ (Brazil), INFN (Italy), MEXT (Japan), SNF (Switzerland), SNF (Denmark), EPSRC (UK) and NSF (US).

REFERENCES

1. M. Amoretti, *et al.*, Nature **419**, 456 (2002)
2. G. Gabrielse, *et al.*, Phys. Rev. Lett. **89**, 213401 (2002)
3. M. Amoretti, *et al.*, Phys. Lett. B. **578**, 23 (2004)
4. M. Amoretti *et al.*, Phys. Lett. B **590**, 133 (2004)
5. N. Madsen, *et al.*, Phys. Rev. Lett. **94**, 033403 (2005)
6. P.D. Bowe, *et al.*, CERN-SPSC-2005-006, SPSC-P-325 (2005)
7. M. Niering, *et al.*, Phys. Rev. Lett. **84**, 5496 (2000).
8. G. Gabrielse, S.L. Rolston, L. Haarsma, W. Kells, Phys. Lett. A **129**, 38 (1988)
9. R.G. Greaves, M.D. Tinkle and C.M. Surko, Phys. Plasmas **1**, 1439 (1994)
10. R. G. Greaves and C. M. Surko, Phys. Rev. Lett. **85**, 1883 (2000)
11. L.V. Jørgensen, *et al.*, Phys. Rev. Lett. **95**, 025002 (2005)
12. G. Gabrielse *et al.*, Phys. Lett. B **507**, 1 (2001)
13. M. Amoretti *et al.*, Phys. Rev. Lett. **91**, 055001 (2003)
14. M. Amoretti *et al.*, Nucl. Inst. & Meth. A **518**, 679 (2004)

15. M. C. Fujiwara *et al.*, Phys. Rev. Lett. **92**, 065005 (2004)
16. S. G. Kuzmin and T. M. O'Neil, Phys. Plas. **12**, 012101 (2005)
17. M. Amoretti *et al.*, Phys. Lett. B **583**, 59 (2004)
18. M.E. Glinsky and T.M. O'Neil, Phys. Fluids B **3**, 1279 (1991)
19. F. Robicheaux, Phys. Rev. A **70**, 022510 (2004)
20. M.H. Holzscheiter and M. Charlton, Rep. Prog. Phys. **62**, 1 (1999)
21. H. A. Bethe and E.E. Salpeter, Quantum Mechanics of One- and Two-Electron Systems (Springer, Berlin, 1957).
22. P. Mansback and J. C. Keck, Phys. Rev. **181**, 275 (1969)
23. J. Stevefelt, J. Boulmer and J-F. Delpech, Phys. Rev. A **12**, 1246 (1975)
24. F. Robicheaux, Phys. Rev. A **73**, 033401 (2006)
25. A. Wolf, Hyp. Int. **76**, 189 (1993)
26. M. Amoretti, *et al.*, Submitted to Phys. Rev. Lett. (2006)
27. J. W. Humberston, M. Charlton, F. M. Jacobsen and B. I. Deutch, J. Phys. B **20**, L25 (1987)
28. C. Storry *et al.*, Phys. Rev. Lett. **96**, 263401 (2004)
29. A. Kellerbauer, *et al.*, Phys. Rev. A. **73**, 062508 (2006)